Journal of Physics: Conference Series

PAPER • OPEN ACCESS

Impact of Cortical Bone Thickness on the Parameters of Fast and Slow Ultrasound Wave based on 2-D Simulation

To cite this article: Muhamad Amin Bin Abd Wahab *et al* 2023 *J. Phys.: Conf. Ser.* **2622** 012008

Impact of Cortical Bone Thickness on the Parameters of Fast and Slow Ultrasound Wave based on 2-D Simulation

Muhamad Amin Bin Abd Wahab[1], Rubita Sudirman[1] and Nasrul Humaimi Mahmood[1]
[1]Faculty of Electrical Engineering, Universiti Teknologi Malaysia, Johor Malaysia.

Email: muhamadamin.abdwahab@utm.my

Abstract. Quantitative Ultrasound (QUS) has been introduced to measure the quality of human bones using ultrasound and become one of the prevention methods for Osteoporosis diseases. Because of the porous composition inherent in human cancellous bone, the generation of both fast and slow waves occurs, and these waves exhibit a distinct association with the cancellous bone structure, particularly the extent of porosity. Nonetheless, the presence of these waves is also contingent upon the anisotropy of cancellous bone, and it is noteworthy that most human cancellous bones are enveloped by cortical bone, which may influence the parameters of the fast and slow waves. Therefore, the aim of this study is to perform a 2-Dimensional (2-D) simulation utilizing the through transmission (TT) measurement method. The primary focus is to examine the impact of cortical thickness on the parameters of both the fast and slow waves. The cortical thickness will be added to the cancellous bone models and the thickness will be varied. Then, the fast and slow wave parameters will be compared in terms of correlation coefficient to identify which wave is affected more. The result shows that the cortical thickness causes increasing in attenuation and velocity for both fast and slow waves. The increase in attenuation is due to sonometry effects while the different longitudinal velocities of water and bone material may contribute to the behaviors for phase velocity measurements. However, the fast wave shows more correlation with the cortical thickness for attenuation (R^2 = 0.76) and phase velocity (R^2 = 0.77) parameters. This is due to fast wave corresponding to the solid structure and increasing cortical thickness also increase the solid structure. Thus, analyzing fast waves against human cancellous bone, cortical bone thickness needs to be considered to ensure accurate measurements.

1. Introduction

Ultrasound systems find extensive usage across various fields, including medicine [1], biology, engineering, and numerous other domains [2]. Using ultrasound technology, Quantitative Ultrasound (QUS) serves as the earliest technique to assess bone quality, serving as a preventive measure against bone loss resulting from Osteoporosis [3]. By analyzing the attenuation and velocity of the ultrasound wave, QUS can predict bone quality [4]. Furthermore, studies have demonstrated that when ultrasound waves traverse a porous structure, they exhibit two distinct categories of longitudinal waves: fast waves and slow waves. The fast wave represents the waves that correspond to the solid trabecular structure, whereas the slow wave represents the wave associated with the porous regions of cancellous bone [5]. Both waves show a high correlation with the microstructure of cancellous bone [6-12]. The discovery offers a potential alternative approach to improve the assessment of bone quality through the utilization of ultrasound for diagnosing bone loss. Nevertheless, the interference between these two wave modes frequently occurs as a result of the significant anisotropy present in cancellous bone [5]. Not only that, most human bone structures are also covered with cortical bone which is a denser type of bone than cancellous bone. The existence of these bones may affect the two modes wave [13]. Therefore, it is necessary to investigate the utilization of the fast and slow waves in the human cancellous bone structure, which is predominantly covered by cortical bone. Thus, the objective of this study is to conduct a 2-Dimensional (2-D) simulation utilizing the through transmission (TT) measurement method to examine the impact of cortical thickness on the parameters of fast and slow waves. One 2-D cancellous bone model sample was used for this investigation and the cortical layer was added and its thickness will be the manipulated variable. Subsequently, the parameters derived from the fast and slow waves will be graphed against cortical bone thickness, and the results, measured in terms of correlation coefficient (R^2), will be compared between the fast and slow waves.

2. Materials and Methods

The 2-D cancellous model employed in this study is a modified version based on previous research conducted by Gilbert et al. [14], specifically focused on cancellous bone and previous works [15, 16]. The porosity of the bone models, which was determined using ImageJ software, is measured to be 66.5%. This measurement involved applying a colour threshold between black and white colours. In Fig. 1 (a), the black colour represents the solid bone structure and the white colour represents the pore structure. The black solid structures at the top and bottom of the cancellous bone model are assumed to be cortical bone and the thickness is labelled as T. The value of T will increase from 0 mm to 3 mm in increments of 0.5 mm. Therefore, the total number of cancellous bone models with different cortical bone thicknesses in this investigation is 7 which are 0 mm, 0.5 mm, 1.0 mm, 1.5 mm, 2.0 mm, 2.5 mm, and 3 mm. The reason for choosing the cortical thickness range of 0 to 3 mm is that the observational limit of fast waves is 3 mm. If the cortical thickness is more than 3 mm, fast waves can no longer be observed.

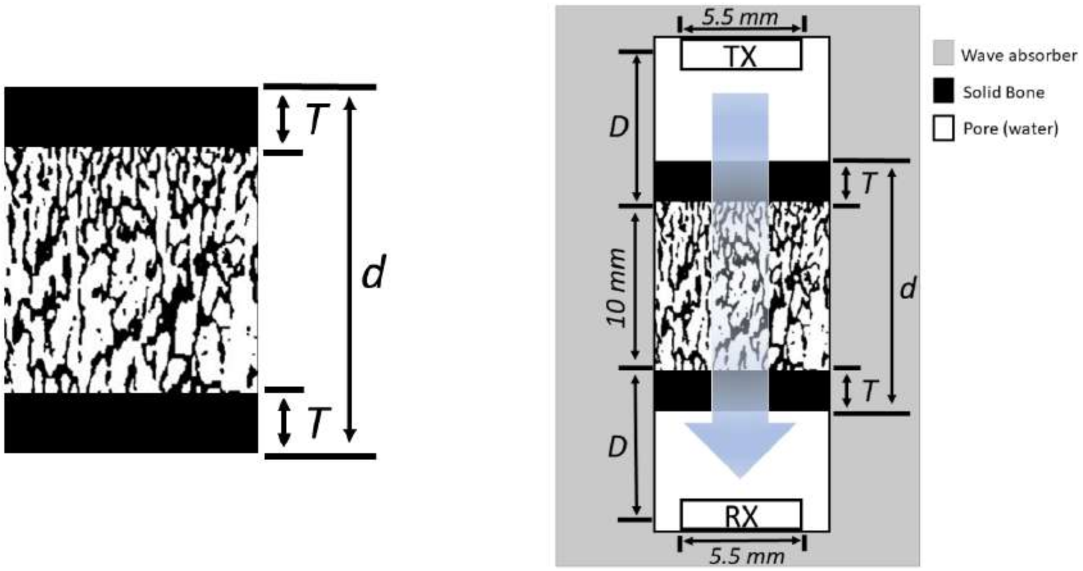

(a) (b)

Figure 1. (a) The 2-D cancellous bone models possess a porosity level of 66.5%. The black and white colour corresponds to solid bone and pore structure. (b) Simulation setup for the correlation of the cortical bone thickness with ultrasound wave investigation. The value of *D* is 8 mm.

2.1. Simulation Setup for Through Transmission Measurement Technique

The simulation software utilized for this investigation is SimNDT software version 0.52 [17]. The simulation configuration was established according to the through transmission (TT) measurement technique, employing a single Gaussian sine wave with a frequency of 1 MHz as the output pulse for the transducer. As depicted in Figure 1(b), the transducer utilized in the study was a planar type with dimensions measuring 5.5 mm. The direction of the wave propagation is from the top (transmitter, TX) to the bottom (receiver, RX) which is also represented by the blue arrow. The simulation duration was established at 25 µs, while the input voltage for the transmitter remained at the default value of 400 volts peak-to-peak (V_{pp}). The distance (D) maintained a constant value of 8 mm between the transducer and the cancellous bone models, excluding the cortical bone layer. In other words, the value of *D* is constant even though the value of *T* is increased. The simulation area was encompassed by an absorbing layer, which had a uniform thickness of 5 mm. The 8 mm is chosen as the D value because of the limitation of the software where it can't be set the distance between the transducer more than 20 mm (including the bone models).

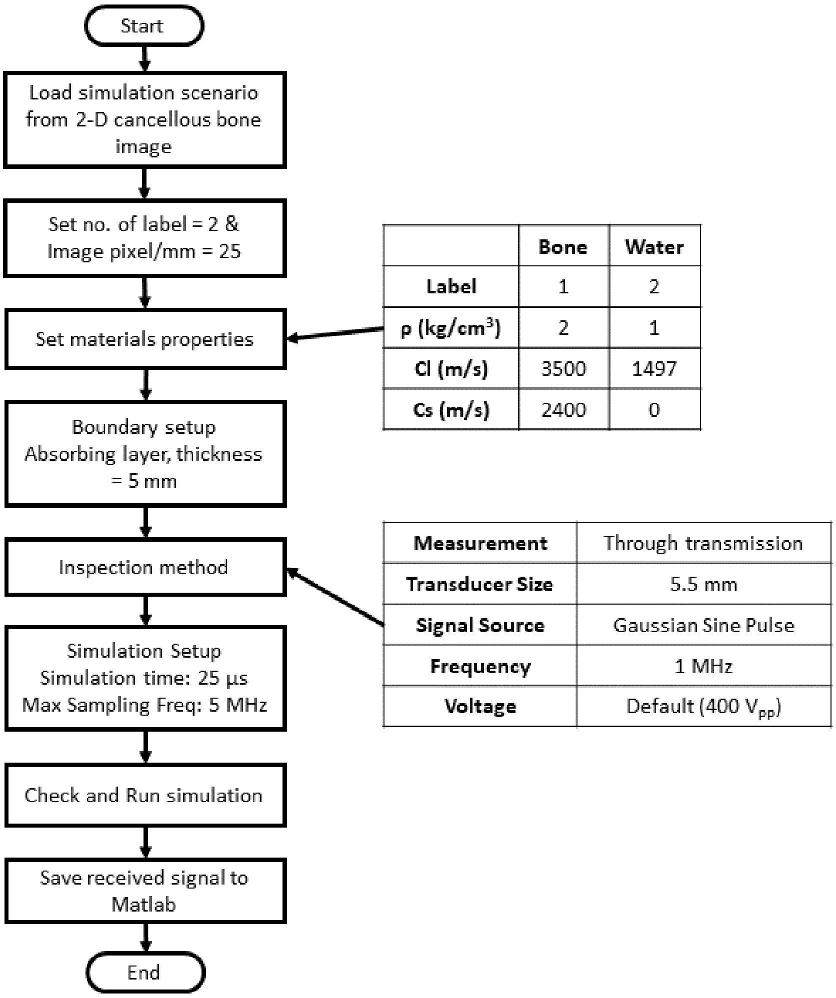

Figure 2. Brief flowchart of the overall simulation process.

Table 1. Materials properties for the simulation.

No.	Material	Colour label	No. Label	ρ (g/cm³)	ϕ	v (m/s)
1.	Water	White	2	1000	-	*Cl*: 1497 *Cs*: 0
2.	Bone	Black	1	2000	66.5%	*Cl*: 3500 *Cs*: 2400

ρ: Density, ϕ: Porosity, v: Velocity, *Cl*: Longitudinal Velocity, *Cs*: Shear Velocity

Table 1 displays the acoustic and material properties of bone and water, sourced from the acoustic properties database available on the internet [18]. The simulation software incorporates the parameter values from Table 1, such as density and velocity, to define the properties of the materials employed. For example, the colour label "white," density of 1 kg/cm³, *Cl* velocity of 1497 m/s, and C_S velocity of 0 m/s correspond to the characteristics of water substance. Furthermore, the geometric scenario of the bone model image was scaled to 170 × 125 pixels, and the simulation software was configured with a scale of 25 pixels per millimeter. For reference waveform acquisition, the simulation setup is also the same as shown in Fig. 1 (b), but the main difference is that there is no sample between TX and RX. The overall simulation process can be referred to in Fig. 2.

2.2. Ultrasound Wave Parameter

This investigation focuses on the ultrasound parameters of attenuation and phase velocity. The calculation of the attenuation, *A* is as follows [16, 19],

$$A(dB) = 20\,log10\left[\frac{S_R(f)}{S_B(f)}\right] \tag{1}$$

the peak amplitude spectrum of the reference wave, denoted as $S_R(f)$, and the peak amplitude spectrum of the sample wave, denoted as $S_B(f)$, are utilized. The resulting amplitude difference A is measured in decibels (dB). Additionally, the phase velocity, $C(f)$, of the wave is calculated using the following formula,

$$C(f) = \frac{c}{1+\frac{p(f)}{2\pi f d}} \tag{2}$$

where, *c* is the temperature-dependent speed of sound in distilled water, 1479 m/s, $p(f)$ is the unwrapped phase difference between the waveform through the sample and the reference waveform and *d* is the sample thickness in mm. The unit for the $C(f)$ is m/s.

3. Result and Discussion

Fig. 3 shows the received reference waveform and the sample waveform for the cortical thickness of 0 mm, 1.5 mm, and 2.5 mm. The second large peak is considered as the peak amplitude of the waveform. Observation on the peak of the sample waveform, the arrival time of the sample waveform is getting quicker when the cortical thickness increases. The arrival time for the reference wave is 17.55 µs and the arrival time for the sample wave with T = 0 mm, T = 1.5 mm and T = 2.5 mm is 17.48 µs, 16.41 µs and 15.63 µs, respectively. In terms of amplitude, the amplitude of the sample wave did not show a clear trend as the cortical thickness increased. The amplitude for the sample wave with T = 0 mm, T = 1.5 mm and T = 2.5 mm is 2.05 V, 0.94 V and 1.11 V, respectively. Moreover, the fast wave can be observed at the arrival time between 13 µs and 15 µs for the sample wave with T = 0. Fig. 4 shows the fast wave for the sample with T = 0 mm, T = 1.5 mm, and T = 2.5 mm.

The sample waveform in Fig. 3 can be assumed as slow wave, while the small waveform located in front of the sample waveform in time domain that was shown in Fig. 4 is fast wave. The fast wave amplitude can be clearly observed in the time domain for the T = 0 mm, however, for the T = 1.5 mm and 2.5 mm, the fast wave amplitude is barely observed. The fast wave amplitude for all the three cortical thickness is 0.1 V, 0.05 V and 0.04 V, respectively. Meanwhile, the fast wave arrival time for all the three cortical thickness is 14.12 µs, 13.29 µs and 12.61 µs, respectively. The fast wave arrival time is also getting quicker when the cortical thickness increases. The findings of this study align well with previous research, which also reported the presence of both fast and slow waves even when the cancellous bone models are surrounded by cortical layers [13]. The observation also aligns with previous works, where typically fast wave has lower amplitude than slow wave [6-11]. Table 2 shows the arrival time of fast and slow wave for every cortical thickness.

Table 2. Arrival time of fast and slow wave.

No.	Cortical Thickness, T (mm)	Slow wave arrival Time (µs)	Slow wave arrival Time (µs)
1.	0	14.12	15.50
2.	0.5	13.97	15.14
3.	1.0	13.41	14.69
4.	1.5	13.29	14.33
5.	2.0	12.78	13.87
6.	2.5	12.61	13.56
7.	3.0	11.94	13.17

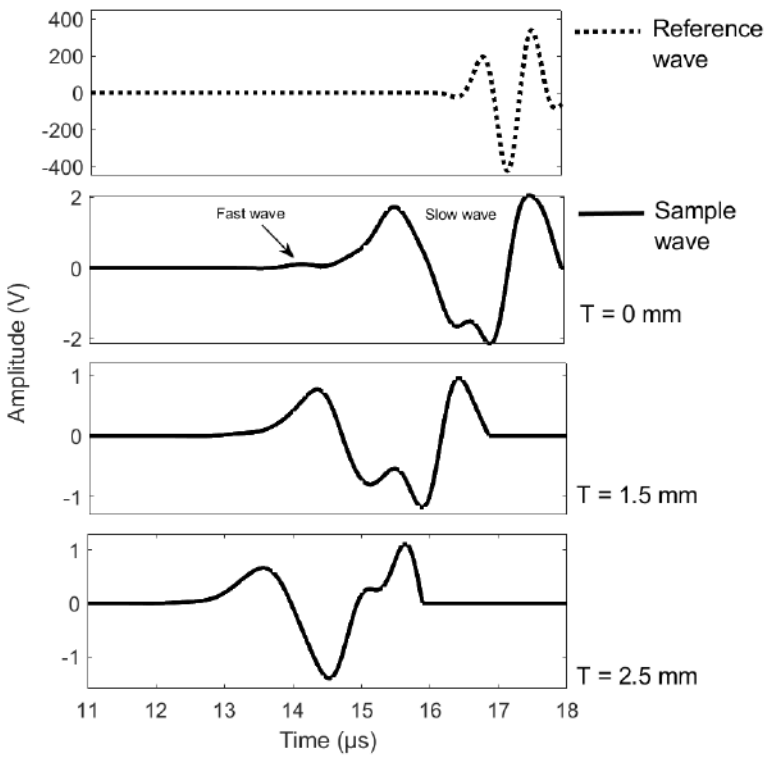

Figure 3. Example of the received waveform from reference wave and sample wave with T = 0 mm, T = 1.5 mm, and T = 2.5 mm, respectively.

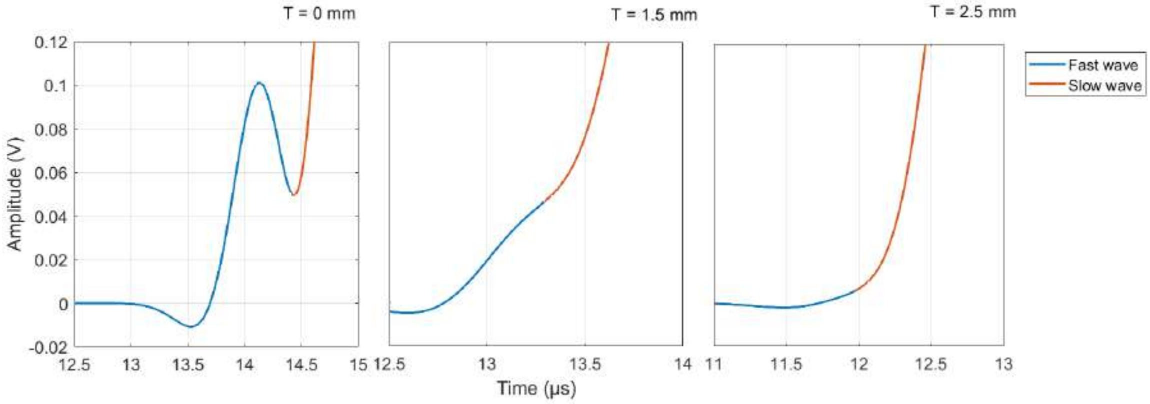

Figure 4. The fast waveform for the sample with T = 0 mm, T = 1.5 mm, and T = 2.5 mm, respectively.

Fig. 5 (a) and (b) shows that, the attenuation value for both fast and slow wave shows an increasing trend versus cortical thickness. Moreover, the R^2 value for the fast wave is 0.76 meanwhile the R^2 value for the slow wave is 0.60. In Fig. 6 (a) and (b) demonstrates that, fast and slow wave phase velocity increase when cortical thickness increase. Comparing the R^2 value, the fast wave ($R^2 = 0.77$) shows slightly significant relation with the cortical thickness compared to slow wave ($R^2 = 0.41$). Overall observation of R^2 values for both fast wave parameters showed a clear correlation with cortical thickness. For slow waves, only the attenuation parameter showed a slightly significant correlation with cortical thickness. The increasing cortical thickness also increases the solid structure of the bone sample and seems to contribute to increasing trends for both fast and slow wave attenuation. The increasing attenuation might be responsible for the negative trend for the amplitude for both fast and slow wave as observed in Fig. 3 and Fig. 4. This behavior is also similar to the case where the low porosity of cancellous bone (increase of the solid structure) has high attenuation properties to fast and slow waves due to sonometry effect [20-22].

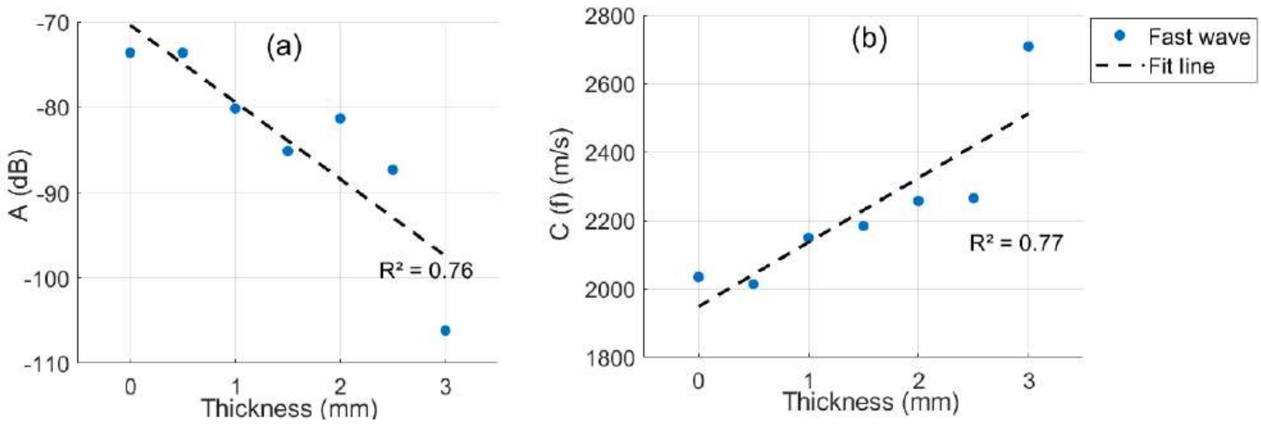

Figure 5. Graphs of the cortical thickness versus ultrasound parameters for (a) *A* and (b) *C(f)* for the fast wave

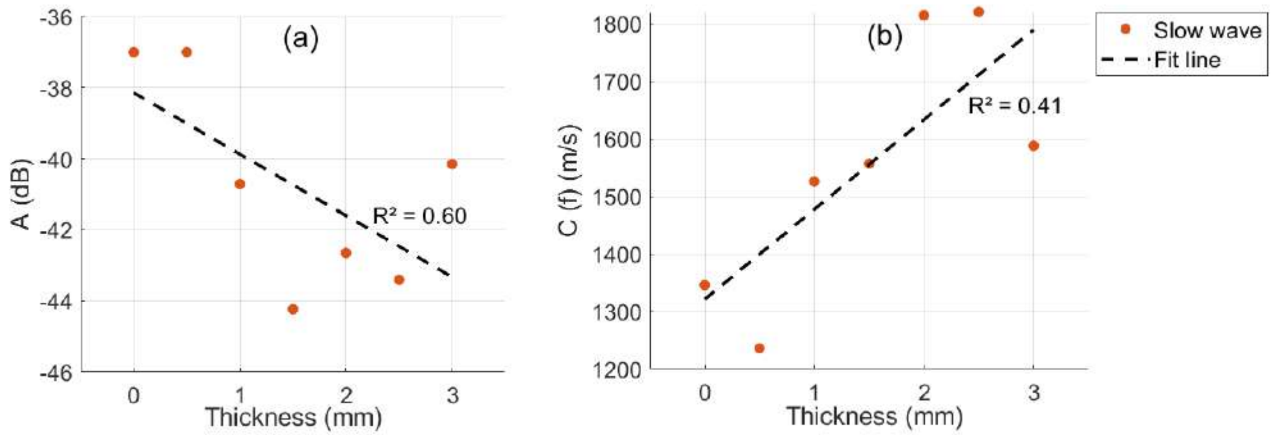

Figure 6. Graphs of the cortical thickness versus ultrasound parameters for (a) *A* and (b) *C(f)* for the slow wave

Table 3. Overall result for attenuation and phase velocity

No.	Wave	Parameters	Correlation Coefficient (R^2)
1.	Fast	Attenuation	0.76
		Phase Velocity	0.77
2.	Slow	Attenuation	0.60
		Phase Velocity	0.41

The phase velocity for both waves also increases when cortical thickness increase. This behavior might be due to the longitudinal velocity, *Cl* of the bone enhance the phase velocity of the ultrasound wave. When the ultrasound wave from the medium with a low *Cl* value, (e.g., water) propagates through the medium with a high *Cl* value (e.g., bone), the wave velocity will rise. In this simulation, the value of the *Cl* for water is to set 1497 m/s meanwhile the value of *Cl* for bone is set to 3500 m/s. With an increase in cortical thickness, the propagation of waves within the bone region becomes more prolonged, consequently leading to an elevation in the phase velocity. Because of this, the arrival time of the sample wave shown in Fig. 3 and Fig. 4 also increases. Nevertheless, the Fig. 5 shows that, cortical thickness correlate more with fast wave compared to slow wave (Fig. 6). This outcome is anticipated as the fast wave emerges from the singular mode wave that spreads through the solid structure of the porous media [8]. Simply put, the fast wave is related to the solid structure, while the slow wave is related to the pores present within the porous structure [23]. Table 3 shows the overall result of the correlation coefficient for attenuation and phase velocity for both fast and slow wave. The outcomes indicate the significance of considering cortical bone thickness when leveraging the benefits of fast waves in ultrasound measurements of human cancellous bone.

4. Conclusion

The effect of the cortical thickness with the two modes wave has been investigated using 2-D ultrasound simulation. Increased cortical thickness correlated positively with the attenuation and the phase velocity parameters. As solid structure increases due to cortical thickness increase, the attenuation and the phase velocity of the wave also increase. However, the increases of the cortical thickness affected more to the fast wave compared to slow wave. This result is expected for fast waves because these waves result from ultrasound waves that are propagated through the solid structure of cancellous bone. Hence, the cortical thickness needs to be considered if the fast wave will be applied for the investigation between ultrasound wave and cancellous bone structure.

Acknowledgments
This work was financially supported by the Malaysia Ministry of Higher Education and Universiti Teknologi Malaysia under the Fundamental Research Grant Scheme R.J130000.7851.5F425 and University Grant Q.J130000.2551.21H49.

References

[1] V. Chijindu, C. Udeze, M. Ahaneku and E. Anoliefo, Bulletin of Electrical Engineering and Informatics **7** (2), 222-229 (2018).
[2] A. C. Toufik Merdjana, International Journal of Power Electronics and Drive System (IJPEDS) **10** (2), 1064 - 1071 (2019).
[3] Q. Grimal and P. Laugier, Irbm **40** (1), 16-24 (2019).
[4] P. Laugier and G. Haïat, *Bone quantitative ultrasound*. (Springer, 2011).
[5] A. Hosokawa, Y. Nagatani and M. Matsukawa, in *Bone Quantitative Ultrasound* (Springer, 2011), pp. 291-318.
[6] A. Hosokawa, Ieee T Ultrason Ferr **62** (6), 1201-1210 (2015).
[7] Y. Nagatani, V.-H. Nguyen, S. Naili and G. Haïat, presented at the 6th European Symposium on Ultrasonic Characterization of Bone (ESUCB) 2015 (unpublished).
[8] S. Kawasaki, R. Ueda, A. Hasegawa, A. Fujita, T. Mihata, M. Matsukawa and M. Neo, J Acoust Soc Am **138** (1), EL83-87 (2015).
[9] T. Otani, Japanese journal of applied physics **44** (6S), 4578 (2005).
[10] L. Cardoso, F. Teboul, L. Sedel, C. Oddou and A. Meunier, Journal of bone and mineral research : the official journal of the American Society for Bone and Mineral Research **18** (10), 1803-1812 (2003).
[11] A. M. Nelson, J. J. Hoffman, M. R. Holland and J. G. Miller, presented at the IEEE International Ultrasonics Symposium, 2012 (unpublished).
[12] Y. Nagatani, K. Mizuno and M. Matsukawa, Ultrasonics **54** (5), 1245-1250 (2014).
[13] A. Hosokawa and Y. Nagatani, Japanese Journal of Applied Physics **51** (7S), 07GF19 (2012).
[14] R. P. Gilbert, P. Guyenne and J. Li, Computers in biology and medicine **45**, 143-156 (2014).
[15] M. A. Abd Wahab, R. Sudirman, M. A. A. Razak, F. K. C. Harun, N. A. A. Kadir and N. H. Mahmood, TELKOMNIKA **18** (4), 1968-1975 (2020).
[16] M. A. A. Wahab, R. Sudirman, M. A. A. Razak and P. I. Khalid, presented at the 2018 2nd International Conference on BioSignal Analysis, Processing and Systems (ICBAPS), 2018 (unpublished).
[17] M. Molero-Armenta, U. Iturrarán-Viveros, S. Aparicio and M. Hernández, Computer Physics Communications **185** (10), 2683-2696 (2014).
[18] Signal-Processing, (Signal-Processing), Vol. 2019.
[19] M. Salim, M. Ahmmad, S. Rosidi, B. Ariffin, I. Ahmad and A. Supriyanto, presented at the Proceeding of The 3rd WSEAS International Conference on Visualization, Imaging and Simulation, 2010 (unpublished).
[20] A. M. Nelson, J. J. Hoffman, C. C. Anderson, M. R. Holland, Y. Nagatani, K. Mizuno, M. Matsukawa and J. G. Miller, J Acoust Soc Am **130** (4), 2233-2240 (2011).
[21] R. P. Gilbert, P. Guyenne and J. Li, Computers & Mathematics with Applications **66** (6), 943-964 (2013).
[22] J. J. Hoffman, A. M. Nelson, M. R. Holland and J. G. Miller, The Journal of the Acoustical Society of America **132** (3), 1830-1837 (2012).
[23] K. I. Lee, The Journal of the Acoustical Society of America **140** (6), EL528-EL533 (2016).